SIN-CHN SCIENTIFIC PRESS PTE.LTD.

Molecular & Cellular Biomechanics 2024, 21(2), 292.
https://doi.org/10.62617/mcb292

Article

The effect of simulated basketball game load on patellar tendon load during stop-jump movement

Dongxu Wang[1], Fengping Li[1], Julien S. Baker[2], Penhui Zhang[1], Zhenghui Lu[3], Jingyao Yu[1], Minjun Liang[1,*]

[1] Faculty of Sports Science, Ningbo University, Ningbo 315211, China
[2] Department of Sport and Physical Education, Hong Kong Baptist University, Hong Kong 999077, China
[3] Faculty of Engineering, University of Pannonia, Veszprem 8201, Hungary
*** Corresponding author:** Minjun Liang, liangminjun@nbu.edu.cn

CITATION

Wang D, Li F, Baker JS, et al. The effect of simulated basketball game load on patellar tendon load during stop-jump movement. Molecular & Cellular Biomechanics. 2024; 21(2): 292.
https://doi.org/10.62617/mcb292

ARTICLE INFO

Received: 13 August 2024
Accepted: 26 August 2024
Available online: 7 November 2024

Abstract: Patellar tendinopathy (PT) is frequently observed among basketball players, particularly in sports involving repetitive jumping movements. However, the overall impact of accumulated exercise load on the patellar tendon is still not fully comprehended. Therefore, the goal of this study is to examine how a simulated basketball game affects the biomechanics of stop-jump movements, specifically focusing on the effects on the patellar tendon. The kinematic and kinetic data were collected immediately after the warm-up and each phase of the simulated basketball game (P1, P2, P3, and P4). A musculoskeletal model was built to calculate patellar tendon force (PTF) and the key biomechanical metrics during the horizontal landing and vertical jumping phases were explored separately, followed by correlation analyses. Linear regression analyses were performed on variables strongly correlated with PTF. The accumulation of load led to significant differences ($p < 0.05$) in the angles, velocities, torques, work contributions, peak patellar tendon force (PTF), and anterior-posterior ground reaction force (APGRF) observed during the landing and vertical jump phases at the hip, knee, and ankle joints. PTF showed strong correlations with knee flexion angle, knee extension angular velocity, ankle plantarflexion angular velocity, and APGRF, with R^2 values of 0.50, 0.58, 0.70, and 0.56, respectively. PTF significantly decreased in P3 and P4, possibly due to the subjects' adaptation and adjustment of their stop-jump posture strategy after load accumulation, including reducing knee and hip flexion angles and decreasing the net knee extension moment.

Keywords: basketball exercise simulation; cumulative exercise load; joint work; musculoskeletal simulation; patellar tendon force; Pearson correlation analysis

1. Introduction

Patellar tendinopathy (PT), known commonly as "jumper's knee", is a prevalent condition among athletes engaged in explosive jumping activities, particularly affecting male athletes [1,2]. The dynamics of landing have been identified as a key factor in PT, hence its moniker "landing knee" [3,4]. Research findings show that the prevalence of PT is as high as 45% among top-tier volleyball players and 32% among elite basketball players [5], which can significantly impair athletic performance and potentially shorten careers. Hence, comprehending the risk factors and mechanisms of PT is crucial for devising effective prevention strategies. Given the complex nature of the causes behind PT, robust evidence regarding external factors such as activity level and internal risk factors is scarce [6–9]. To reduce the incidence of PT, pinpointing the factors that predispose individuals to this condition is essential.

The knee joint plays a crucial role in transmitting load and absorbing mechanical energy during the landing process [10]. The patellar tendon serves as a critical conduit

for load transmission during the landing phase [10], facilitating the distribution of kinetic energy to the lower limb joints [11]. This function is acknowledged as a significant biomechanical contributor to the development of PT. Research has indicated that during a stop-jump task, the peak patellar tendon force (PTF) exerted on the patellar tendon can reach up to six times the body weight when landing horizontally, and five times the body weight during vertical landing, as noted in a prior study [12]. This underscores the correlation between landing patterns and the susceptibility to knee joint injuries [12,13]. Studies have revealed notable disparities in the movement dynamics of the lower limbs during the execution of jumping and landing activities, distinguishing those afflicted with PT from their healthy counterparts [14–16]. A recent comprehensive analysis points to the mechanics of knee and hip joint flexion during jumping as closely linked to the risk factors for PT. It is recommended that evaluations of these mechanics should cover the entire jump-landing sequence, including horizontal landings, and be carried out in a prospective manner to pinpoint potential risk factors [17,18]. These insights suggest that horizontal landings are particularly effective for detecting risk factors associated with PT during stop-jump movements. Therefore, in this study, the stop-jump was chosen because it is a common jumping action in basketball that incorporates a horizontal landing phase, which leads to higher patellar tendon loads compared to the vertical jumps [19].

On the other hand, the repetitive stress on the patellar tendon is viewed as an external risk factor for the development of PT [20]. The accumulation of high eccentric tendon loading is believed to induce microtrauma within the tendon, potentially leading to histopathological changes [21]. The ability of tendons to return to their original length after being stretched and released may exhibit significant lag under repeated load, potentially affecting its function. However, this phenomenon has not been definitively validated in the context of the patellar tendon [22]. Knee joint injuries, caused by repetitive stress on the tendon due to overuse, occur more frequently in the latter half of games or during the later stages of competition [23,24]. Therefore, monitoring patellar tendon load in athletes under conditions of accumulated load is crucial. However, the connection between how exercise load accumulates and its impact on the load on the patellar tendon is not yet fully understood [22]. This study seeks to determine whether the accumulation of exercise load can alter patellar tendon load and explore related key factors. By examining the interaction between exercise load and patellar tendon load, as well as the correlation between PTF and other kinematic and kinetic indicators, we can better identify risk factors and explore new methods to prevent PT injuries. The study hypothesizes that as the game progresses and exercise load accumulates, athletes might adjust their landing techniques, potentially leading to a reduction or variation in patellar tendon load. Adjusting landing strategies to reduce patellar tendon load could potentially decrease the incidence of patellar tendon disorders.

2. Methods

2.1. Subjects

A priori power analysis was performed utilizing the G*Power software (version 3.1.9.7, University of Kiel, Kiel, Germany). Based on preliminary data published by

regarding the effect of knee joint angle on patellar tendon stress (effect size $f = 0.40$) [25], the minimum required sample size for conducting repeated measures ANOVA was determined to be 12 ($\alpha = 0.05$, $\beta = 0.2$). In this research, a group of 16 male amateur basketball players was enrolled from local university, as shown in **Table 1**. All participants were right-leg dominant, had normal foot and ankle morphology, and no lower limb injuries in the past 6 months. Knee joint pain was excluded through single leg decline squat (SLDS) tests [26]. A skilled radiologist specializing in musculoskeletal imaging assessed each participant's patellar tendon. Utilizing a 13 MHz linear array ultrasound transducer (Siemens Antares, Siemens AG, Germany), the tendon morphology was determined to be "normal," with no abnormalities detected through ultrasound examination. Before initiating data collection, written informed consent was secured from all participants. The study protocol was approved and accepted by the University's Ethics Committee (RAGH20231105).

Table1. Information of the eligible participants.

Variables	Participants
Number	16
Age (yrs)	22.8 ± 2.0
Height(m)	1.82 ± 0.07
Weight (kg)	77.1 ± 3.1
BMI (kg/m^2)	23.5 ± 2.0
Basketball experience (yrs)	4.9 ± 2.1
Position of play	Point Guard

2.2. Procedures

The study was carried out in the Sports Biomechanics Laboratory at the Institute of Health Science. The movement performed was the stop-jump as illustrated in **Figure 1A**, which is commonly seen in basketball activities such as jump shots [4]. The day before the test, participants underwent a standardized dynamic warm-up for 5 min. Subsequently, they performed three maximal effort stop-jumps, with a 30-second interval between each test, and the jump height was set at 85% of their maximum reach. On the test day, participants completed a 5-minute standardized dynamic warm-up, which included both full-body dynamic and static stretching [27]. This was followed by a 40-minute Basketball Exercise Simulation Test (BEST), divided into four 10-minute stages. During the rest periods immediately following each stage of BEST, three-dimensional motion biomechanics (kinematics and kinetics) and surface electromyography (EMG) data were collected for the stop-jump movements.

In this research, the stop-jump movement was examined during its two distinct phases: the horizontal landing phase and the vertical jumping phase [4]. Initially, participants took a step forward from a self-selected distance, landing each foot on separate force platforms. They then performed a vertical jump, touching a ball on the ceiling with their dominant hand; the ball was positioned directly above the force platforms. Before the experiment, professional basketball players provided demonstrations and explanations of the movements to ensure that all participants had

a thorough understanding of the task, thereby guaranteeing consistency in data collection. A successful stop-jump required (1) complete foot contact with the force platform and (2) touching the ball on the ceiling. Participants were required to perform the stop-jump five times, with the middle three trials used for subsequent analysis. All subjects wore their own athletic shoes during the experiment [4,25].

2.3. Basketball exercise simulation test

The BEST is a basketball-related training test designed to replicate the physical demands of a basketball game. The duration of BEST strictly follows official game timings, divided into four identical 10-minute intervals of specific intermittent exercises. There is a 3-minute rest between the first and second intervals and between the third and fourth intervals, with a 15-minute halftime rest. Each BEST cycle consists of 30 s of intermittent specific exercises, incorporating a combination of sprints, jumps, runs, jogs, shuffles, and recovery [27]. **Figure 1B** depicts the various activities and distances undertaken throughout each cycle of the BEST protocol. Participants start each cycle from a standstill, with each BEST cycle constrained to 30 s, requiring continuous execution within each 10-minute interval (allowing for up to 20 cycles per interval). Participants usually finish each cycle in 25 s, allowing for a minimum of 5 s of rest before starting the subsequent cycle. If participants cannot complete a cycle within the allotted time, they must stop entirely and immediately begin the next cycle.

2.4. Data collection and processing

All participants were fitted with 37 reflective markers, each 12.5mm in diameter. **Figure 1C** shows the placement of each marker, a method previously validated in earlier research [28,29]. Marker trajectories were recorded with a Vicon system (Oxford Rolling Limited, UK), which utilized 10 cameras running at a 200 Hz frequency. Simultaneously, the ground reaction forces were captured at a 2000 Hz frequency employing a force platform (Kistler, Switzerland). Muscle activity was recorded using the EMGworks Acquisition system (Delsys, Boston, MA, USA) at a frequency of 1000 Hz, capturing EMG signals from the rectus femoris (RF), vastus lateralis (VL), vastus medialis (VM), biceps femoris (BF), semitendinosus (ST), tibialis anterior (TA), medial gastrocnemius (MG), and peroneus longus (PL) muscles, as shown in **Figure 1C**. The collection of kinematic, kinetic, and surface EMG data was performed using a synchronizer to ensure signal synchronization. Following the data capture, the kinematic and kinetic data of the participants were exported in the c3d file format using the Vicon software [30]. Data were then further processed using MATLAB R2023a (The MathWorks, Natick, MA, USA). This processing included steps such as coordinate transformation, application of a low-pass filter, extraction of relevant data, and conversion of data formats [31]. The kinematic and kinetic data's coordinate system was aligned to fulfill the specifications necessary for subsequent simulation processes. A fourth-order zero-lag Butterworth low-pass filter was utilized for smoothing the kinematic data and the ground reaction force (GRF) data, with the cutoff frequencies designated at 10 Hz for the kinematic data and 20 Hz for the GRF data. After processing, the data were transformed into the trc format (marker

trajectories) and the mot format.

The initial contact was determined by the vertical ground reaction force (VGRF) exceeding 25 N, while a VGRF below 25 N was defined as the moment of leaving the ground [25]. The horizontal landing phase was delineated as the period from initial foot-ground contact to the point when the knee flexion angle reached its maximum. The vertical jumping phase was demarcated as the period from maximum knee flexion to the point when the VGRF recorded by the force platform fell below 25 N. The peak PTF was identified as the utmost PTF during the landing phase, and all kinetic data were normalized to body weight (BW).

The flexion of the knee and hip joints, along with dorsiflexion of the ankle joint, were categorized as positive movements, whereas the extension of the knee and hip joints, and plantarflexion of the ankle joint, were categorized as negative movements. Negative work values (horizontal landing phase) indicate energy dissipation through eccentric muscle contractions. Additionally, the percentage of energy dissipation by each joint (ankle, hip, and knee) is calculated to understand their respective contributions to the total energy loss [32]. Positive work (vertical jumping phase) values indicate energy output.

Although data from both legs were collected and analyzed, statistical analysis was conducted only on the left lower limb. In basketball, the non-dominant leg is more frequently used for jumping and landing during layups [33]. Most previous studies on patellar tendon force have focused primarily on the dominant leg [4,19,25], with relatively few studies examining the non-dominant leg. Previous research found that among participants classified as having unilateral patellar tendinopathy (PT), 29% had PT in the non-dominant leg, and up to 14% had PT specifically in the non-dominant leg [34]. Given that the non-dominant leg may endure greater forces due to its increased reliance and load [35], this study seeks to explore the effects of load accumulation on patellar tendon loading in the non-dominant leg of basketball players. Only sagittal plane data were included in the statistical analysis, as previous studies have confirmed that the risk of PT is highest in the sagittal plane [14,15].

2.5. Musculoskeletal model

This study utilized an enhanced musculoskeletal model [36], that includes the patella and patellar tendon into the skeletal structure [37]. The model encompasses the trunk and lower limbs, featuring a pelvis with six degrees of freedom and a hip joint designed as a ball-and-socket joint, which allows for three degrees of freedom. Additionally, the ankle, subtalar, and metatarsophalangeal joints are modeled as hinge joints, and the flexion angle of the knee determines the relative movement between the tibia and patella [36]. In the model, the patella is linked to the femur, with the quadriceps muscle enveloping the patella and extending to the tibial tuberosity, as depicted in **Figure 1D**. The patella acts as a smooth pulley, directing the force from the quadriceps muscle along the path of the patellar tendon [37].

In OpenSim v4.4, we followed the standard procedures outlined by Delp [36] to process the data. First, we applied an 18 Hz low-pass filter using a zero-phase fourth-order Butterworth filter to the marker trajectories and ground reaction forces. Next, we scaled the model based on static marker positions and anthropometric data derived

from body weight measurements. The attachment points of the muscles and the lengths of their moment arms were customized to align with the individual limb proportions of each participant [37]. Using the inverse kinematics (IK) algorithm, we determined the joint angles by reducing the differences between the virtual markers in our model and the actual marker trajectories obtained from the experiments. Additionally, we utilized the inverse dynamics (ID) method to calculate the torques at each joint [36]. In this study, we used a weighted static optimization (STO) technique to estimate muscle activation levels and forces, and we validated the reliability of the model-simulated muscle activations using EMG signals.

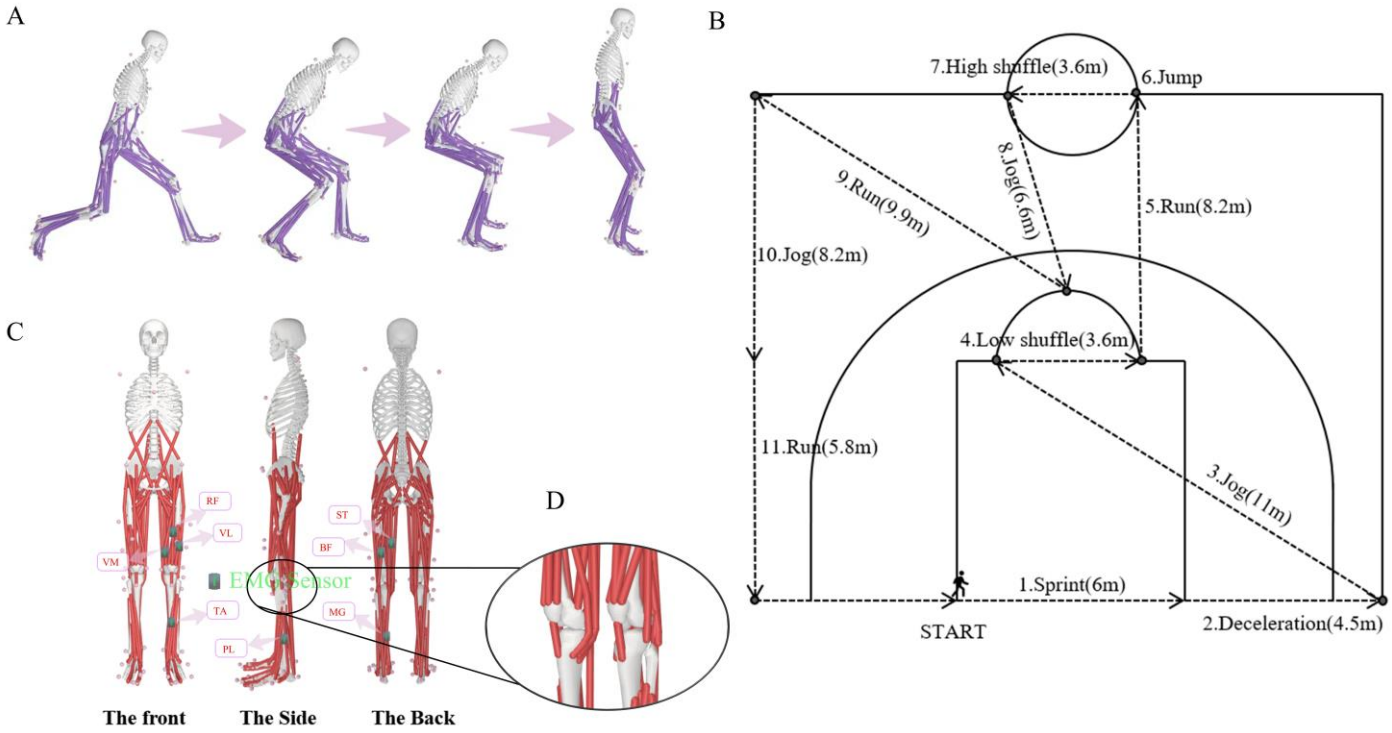

Figure 1. (A) Illustration of the motion capture process; **(B)** a schematic depiction of the Basketball Exercise Simulation Test. **(C)** static marker positions and EMG marker location; **(D)** illustration of the musculoskeletal model, forces in the quadriceps are transmitted through the patella to the tibia; High = high-intensity; Low= low-intensity.

2.6. Statistical analysis

To thoroughly comprehend the time-series variations in patellar tendon loading during the stop-jump, we used the open-source Statistical Parametric Mapping 1D (SPM 1D) package [38], which interprets variability in the data based on random field theory. Statistical analyses were conducted using MATLAB R2023a (The MathWorks, MA, USA). Results were displayed as mean ± standard deviation (SD). For the statistical analysis of discrete outcome variables, we used IBM SPSS Statistics 26. Before performing statistical analysis, a Shapiro-Wilk test for normality was conducted to verify that the data adhered to the assumption of normal distribution. The Mauchly test was used to assess the assumption of sphericity in the variance analysis. If the sphericity assumption was not met ($p < 0.05$), the Greenhouse-Geisser correction was implemented to adjust the degrees of freedom in the analysis. Finally, one-way repeated measures ANOVA was used to test within-subject effects across different

stages of biomechanical indices, including effect size assessment, descriptive statistics, and pairwise comparisons. A significance level of $p < 0.05$ was used throughout the analyses.

A Pearson correlation analysis was conducted to explore the correlation between PTF and various other biomechanical measures. This article only reports the indicators that are significantly correlated with the patellar tendon force ($R > 0.49$). The interpretation of these correlations was based on definitions from previous studies [39]. The square of the Correlation Coefficient R^2 is categorized as follows: values in the range [0.00, 0.01) indicate a negligible correlation, [0.01, 0.16) suggest a weak correlation, [0.16, 0.49) denote a moderate correlation, [0.49, 0.81) signify a strong correlation, and [0.81, 1.00) represent a very strong correlation.

3. Results

3.1. Musculoskeletal model validation

Muscle EMG signals were employed to confirm the muscle activation patterns predicted by the model (**Figure 2**). The EMG data and musculoskeletal simulation data were standardized using z-score normalization, and the consistency between the two measurement methods was visualized using Bland-Altman plots [40]. Among the points, 7.9% were outside the 95% limits of agreement (LoA). The maximum discrepancy within the acceptable range between the two data sets was 0.039, while the average discrepancy was 0.0002.

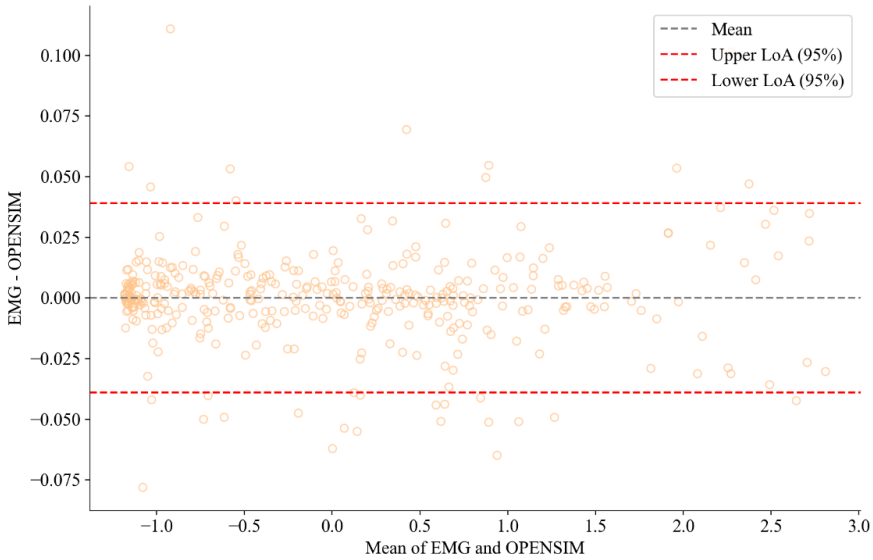

Figure 2. Validation of the opensim musculoskeletal model.

Note: The upper and lower bounds of the 95% Limits of Agreement (LoA) for the mean difference are represented by the upper and lower red dashed lines, respectively, while the grey dashed line represents the 95% Confidence Interval (CI) for the average difference between the two measurement methods.

3.2. Kinematics

Table 2 shows the maximum flexion angles, extension angles, and corresponding angular velocities of the hip, knee, and ankle joints during stop-jump movements in the athletes.

3.2.1. Horizontal landing phase

The maximum hip flexion angle showed significant within-subject effects ($p < 0.001$). The highest value was observed at baseline (warm-up) at 76.32°. The values for P2, P3, and P4 were 72.84°, 72.44°, and 72.04°, respectively, all significantly lower than baseline ($p < 0.05$). Compared to P1, P3 and P4 decreased by 2.54° and 2.94°, respectively, showing significant differences ($p < 0.05$). No significant differences were observed in maximum hip flexion angular velocity.

The maximum knee flexion angle also showed significant within-subject effects ($p < 0.05$). Compared to P1, the maximum knee flexion angles in P2, P3, and P4 were 92.18°, 92.57°, and 90.53°, respectively, all significantly lower than P1 ($p < 0.05$). P4 was significantly lower than P3 by 2.04° ($p < 0.05$). The maximum knee flexion angular velocity showed significant within-subject effects ($p < 0.05$). Knee angular velocities at baseline, P1, and P2 were 8.87 rad/s, 9.22 rad/s, and 10.46 rad/s, respectively, with P2 reaching the peak value of 10.46 rad/s, significantly higher than both baseline and P1 by 1.77 rad/s and 1.24 rad/s, respectively ($p < 0.05$).

The maximum angle of ankle dorsiflexion showed significant within-subject effects ($p < 0.05$). The highest value at P4 was 28.49°. The values at baseline, P1, and P2 were 24.53°, 25.00°, and 26.41°, respectively, all significantly lower than P4 ($p < 0.05$). The maximum ankle dorsiflexion angular velocity showed significant within-subject effects ($p < 0.001$). The values at baseline, P1, P2, and P4 were 4.84 rad/s, 4.80 rad/s, 5.75 rad/s, and 5.84 rad/s, respectively, with P4 reaching the peak value of 5.84 rad/s, significantly higher than baseline, P1, and P2 ($p < 0.001$). Compared to baseline and P1, P2 increased by 0.91 rad/s and 0.95 rad/s, respectively ($p < 0.05$).

3.2.2. Vertical landing phase

During the vertical jumping phase, the maximum angle of hip extension showed no significant differences. The maximum hip extension angular velocity showed significant within-subject effects ($p < 0.05$), reaching a peak of 8.30 rad/s at P2. Compared to P2, the value at P4 decreased by 0.54 rad/s ($p < 0.05$).

The maximum knee extension angle showed no significant differences. The maximum knee extension angular velocity exhibited significant within-subject effects ($p < 0.05$), with P3 showing a decrease of 0.74 rad/s compared to baseline (14.82 rad/s at baseline and 14.08 rad/s at P3, $p < 0.05$).

The maximum ankle plantarflexion angle showed significant within-subject effects ($p < 0.05$). The values at P2, P3, and P4 were 22.68°, 20.86°, and 21.86°, respectively, all significantly lower than baseline ($p < 0.05$). The maximum angular velocity of ankle plantarflexion did not show significant differences.

Table2. Peak angles and velocities of the Hip, Knee, and Ankle during BEST.

Variable	Peak	Baseline	Time point				η^2	*p*-value
			P1 post	P2 post	P3 post	P4 post		
		Mean ± SD	Mean ± SD	Mean ± SD	Mean ± SD	Mean ± SD		
Hip Angle (°)	FLEX (+)	76.32 ± 4.44	74.98 ± 5.83	72.84 ± 5.79*	72.44 ± 5.47*†	72.04 ± 5.19*†	0.66	0.000
	EXT (−)	21.13 ± 2.92	21.22 ± 3.20	20.61 ± 4.68	20.67 ± 5.10	20.88 ± 4.15	0.028	0.936
Knee Angle (°)	FLEX (+)	93.17 ± 5.59	94.06 ± 4.43	92.18 ± 5.16†	92.57 ± 6.57†	90.53 ± 7.08†§	0.47	0.01
	EXT (−)	24.32 ± 5.07	24.08 ± 3.96	24.61 ± 4.32	24.77 ± 4.18	25.68 ± 3.75	0.16	0.453

Table2. (*Continued*).

Variable	Peak	Baseline	Time point				η^2	*p*-value
			P1 post	P2 post	P3 post	P4 post		
		Mean ± SD	Mean ± SD	Mean ± SD	Mean ± SD	Mean ± SD		
Ankle Angle (°)	DF (+)	24.53 ± 5.13	25.00 ± 4.91	26.41 ± 4.24	26.82 ± 4.60	28.49 ± 3.31*†‡	0.61	0.001
	PF (−)	25.47 ± 3.37	23.17 ± 2.54	22.68 ± 3.38*	20.86 ± 3.85*	21.86 ± 4.00*	0.407	0.027
Hip Velocity (rad/s)	FLEX (+)	5.78 ± 1.40	6.30 ± 1.04	5.81 ± 0.58	5.72 ± 0.91	6.10 ± 0.85	0.137	0.542
	EXT (−)	8.01 ± 1.30	8.21 ± 1.10	8.30 ± 1.50	7.80 ± 1.36	7.76 ± 1.09‡	0.321	0.034
Knee Velocity (rad/s)	FLEX (+)	8.87 ± 1.45	9.22 ± 1.48	10.46 ± 1.53*†	9.66 ± 2.43	9.73 ± 2.65	0.396	0.032
	EXT (−)	14.82 ± 1.74	14.55 ± 1.14	14.57 ± 1.31	14.08 ± 1.46*	14.34 ± 1.36	0.414	0.024
Ankle Velocity (rad/s)	DF (+)	4.84 ± 0.80	4.80 ± 0.36	5.75 ± 0.57*†	5.35 ± 0.80‡	5.84 ± 0.94*†§	0.422	0.000
	PF (−)	16.96 ± 1.83	16.53 ± 1.13	16.74 ± 1.81	16.51 ± 1.40	16.65 ± 1.83	0.094	0.724

Note: Phases 1 (P1), 2 (P2), 3 (P3) and 4 (P4); *, †, ‡, § indicate significant differences compared to P0, P1, P2, and P3, respectively ($p < 0.05$). FLEX: flexion; EXT: extension; DF: dorsiflexion; PF: plantar flexion; Data are mean (± standard deviation).

3.3. Kinetics

Table 3 displays the peak joint torques of the hip, knee, and ankle joints, peak VGRF, peak APGRF (anterior-posterior ground reaction force), and peak PTF during stop-jump movements in the athletes.

Table 3. Peak PTF, GRF, and peak hip, knee, and ankle joint moment during BEST.

Variable	Peak	Baseline	Time point				η^2	*p*-Value
			P1 post	P2 post	P3 post	P4 post		
		Mean ± SD	Mean ± SD	Mean ± SD	Mean ± SD	Mean ± SD		
Peak PTF (KG × BW^{-1})	FLEX (+)	1.33 ± 0.14	1.32 ± 0.12	1.34 ± 0.12	1.26 ± 0.13‡	1.23 ± 0.13‡	0.408	0.027
	EXT (−)	1.34 ± 0.15	1.33 ± 0.19	1.38 ± 0.17	1.34 ± 0.19	1.28 ± 0.17‡	0.504	0.017
Peak VGRF（KG × BW^{-1}）	FLEX (+)	1.60 ± 0.18	1.60 ± 0.17	1.63 ± 0.17	1.63 ± 0.16	1.64 ± 0.18	0.255	0.186
	EXT (−)	1.47 ± 0.16	1.47 ± 0.22	1.41 ± 0.12	1.43 ± 0.08	1.46 ± 0.11	0.091	0.734
Peak APGRF（KG × BW^{-1}）	FLEX (+)	0.33 ± 0.10	0.33 ± 0.09	0.33 ± 0.05	0.32 ± 0.05	0.32 ± 0.07	0.068	0.831
	EXT (−)	0.27 ± 0.04	0.26 ± 0.04	0.23 ± 0.02*	0.25 ± 0.04	0.26 ± 0.04‡	0.351	0.039
Hip Moment（N × m × BW^{-1}）	FLEX (+)	2.53 ± 0.67	2.46 ± 0.34	2.71 ± 0.46	2.83 ± 0.67*†	3.29 ± 0.56*†‡§	0.417	0.025
	EXT (−)	0.52 ± 0.37	0.48 ± 0.32	0.56 ± 0.28	0.42 ± 0.22	0.40 ± 0.20	0.134	0.555
Knee Moment （N × m × BW^{-1}）	FLEX (+)	2.65 ± 0.36	2.50 ± 0.32	2.39 ± 0.27*	2.47 ± 0.36	2.31 ± 0.32*†	0.394	0.034
	EXT (−)	0.31 ± 0.11	0.36 ± 0.12	0.34 ± 0.09	0.32 ± 0.08	0.28 ± 0.13†	0.398	0.031
Ankle Moment（N × m× BW^{-1}）	DF (+)	0.30 ± 0.14	0.34 ± 0.11	0.39 ± 0.11	0.33 ± 0.10	0.41 ± 0.20*§	0.419	0.025
	PF (−)	1.96 ± 0.43	1.90 ± 0.36	1.95 ± 0.30	2.02 ± 0.24	1.97 ± 0.29	0.159	0.458

Note: Phases 1 (P1), 2 (P2), 3 (P3) and 4 (P4); PTF: patellar tendon force; VGRF: vertical ground reaction force; APGRF: anterior-posterior ground reaction force; FLEX: flexion; EXT: extension; DF: dorsiflexion; PF: plantar flexion; *, †, ‡, § indicate significant differences compared to P0, P1, P2, and P3, respectively ($P < 0.05$). Data are mean (± standard deviation).

3.3.1. Horizontal landing phase

No significant variations were observed in the VGRF and APGRF across different stages. The peak PTF showed significant within-subject effects ($p < 0.05$). The highest and lowest peak PTF values were observed at P2 (1.34 KG × BW^{-1}) and P4 (1.24 KG × BW^{-1}), respectively, with P4 showing a significant decrease of 0.1 KG × BW^{-1} compared to P2 ($p < 0.05$). As shown in **Figure 3**, P2 was significantly higher than Baseline during the 58%–62% phase, higher than P1 during the 58%–61% phase,

higher than P3 during the 56%–62% phase, and higher than P4 during the 58%–62% phase (all $p < 0.05$).

The maximum hip flexion moment exhibited significant within-subject effects ($p < 0.05$). Significant differences were found between the baseline (2.53 N × m × BW^{-1}) and P1 (2.46 N × m × BW^{-1}) compared to P3 (2.83 N × m × BW^{-1}, $p < 0.05$). At P4, the maximum hip flexion moment reached its highest value (3.29 N × m × BW^{-1}), which was significantly different from the baseline, P1, P2, and P3 (all $p < 0.05$).

The maximum knee flexion moment showed significant within-subject effects ($p < 0.05$). There were significant differences between the baseline (2.65 N×m×BW^{-1}) and P2 (2.39 N × m × BW^{-1}) compared to P4 (2.31 N × m × BW^{-1}, $p < 0.05$). P4 also showed significant differences when compared to both the baseline and P2 ($p < 0.05$).

The maximum ankle dorsiflexion moment showed significant within-subject effects ($p < 0.05$). Significant differences were observed at P4 compared to the baseline (0.41 N × m × BW^{-1}), P3 (0.33 N × m × BW^{-1}), and P3 (0.30 N × m × BW^{-1}) (all $p < 0.05$).

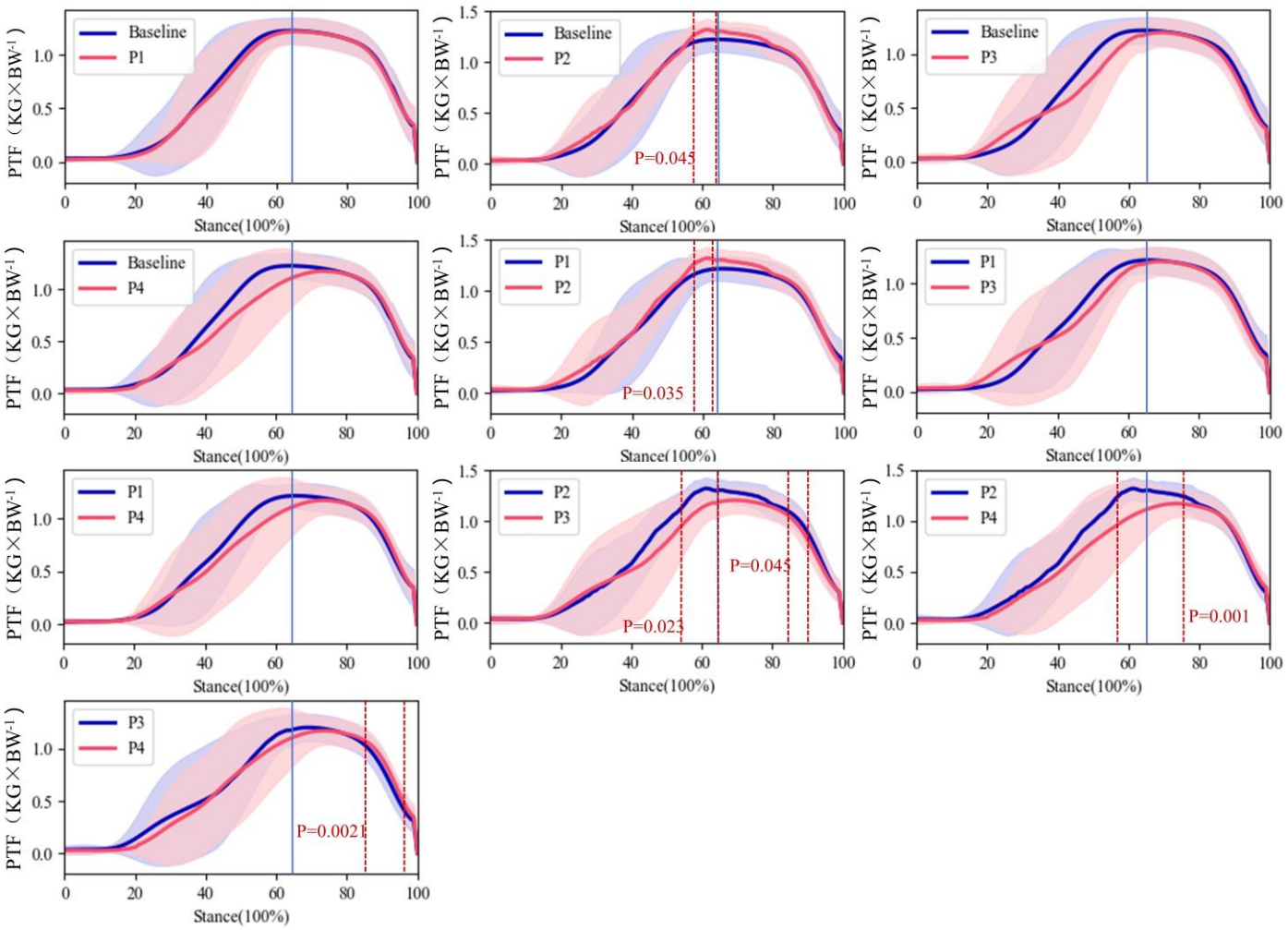

Figure 3. A comparative analysis of the forces exerted on the patellar tendon during distinct phases of stop-jump movement in basketball simulated games was conducted using SPM. The red dashed areas indicate statistically significant differences. The 0–100 scale below each image represents the stop-jump phase. In each image, the initial phase (0%) to the solid blue line represents the horizontal landing phase, while the phase from the solid blue line to the end (100%) represents the vertical take-off phase.

3.3.2. Vertical landing phase

No significant differences in VGRF at different stages. The APGRF was 0.27 KG × BW^{-1} at baseline and 0.23 KG × BW^{-1} in P2, showing a decrease of 0.04 KG × BW^{-1} ($p < 0.05$). P4 increased by 0.03 KG × BW^{-1} compared to P2 ($p < 0.05$).

The peak PTF reached its maximum and minimum values in P2 and P4, respectively, at 1.38 KG × BW^{-1} and 1.28 KG × BW^{-1}. P4 showed a decrease of 0.1 KG × BW^{-1} compared to P2 ($p < 0.05$). As clearly shown in **Figure 3**, P2 was significantly higher than P3 between 82%–90% ($p < 0.05$). Compared to P4, P2 was significantly higher between 64%–76% ($p < 0.05$). Compared to P4, P3 was significantly higher between 82%–95% ($p < 0.05$).

No significant differences in the maximum hip and ankle extension torque. The maximum knee extension moment at P1 and P4 were 0.36 N × m × BW^{-1} and 0.28 N × m × BW^{-1}, respectively, with a significant decrease of 0.08 N × m × BW^{-1} ($p < 0.05$).

3.4. Joint work

3.4.1. Horizontal landing phase

Figure 4 illustrates the overall and relative work done by the joints. The total eccentric work performed by the joints exhibited a significant primary effect ($p < 0.05$). The total eccentric work at baseline, P1, and P2 were 2.28 J/kg, 2.48 J/kg, and 2.46 J/kg, respectively, with P1 and P2 being significantly higher than baseline ($p < 0.05$) (**Figure 4A**).

In terms of relative joint work, there was a significant primary effect observed specifically in the work done by the hip joint. ($p < 0.05$). Compared to baseline, the hip joint's contribution to work at P4 significantly increased by 3.14% ($p < 0.05$). The knee joint also showed a significant main effect ($p < 0.05$). Compared to baseline, the knee joint's contribution to eccentric work at P4 significantly decreased by 4.09% ($p < 0.05$). No significant differences were noted in the ankle joint work across different load stages.

3.4.2. Vertical landing phase

The total concentric work of the joints showed a significant main effect ($p < 0.05$), with values of 3.85 J/kg, 3.63 J/kg, and 3.56 J/kg for P1, P2, and P4, respectively. Both P2 and P4 were significantly lower than P1 ($p < 0.05$) (**Figure 4B**).

Regarding relative joint work, the hip joint showed a significant primary effect ($p < 0.05$). Compared to baseline, the hip joint's contribution to work significantly decreased by 4.69% ($p < 0.05$) (**Figure 4C** and **Figure 4D**). The knee joint also exhibited a significant main effect ($p < 0.05$), with its contribution to work increasing by 5.06% compared to baseline ($p < 0.05$) (**Figure 4C** and **Figure 4D**). The ankle joint's concentric work showed a significant main effect ($p < 0.05$), with contributions of 32.62% and 35.97% at P2 and P4, respectively, representing a significant increase of 3.35% ($p < 0.05$).

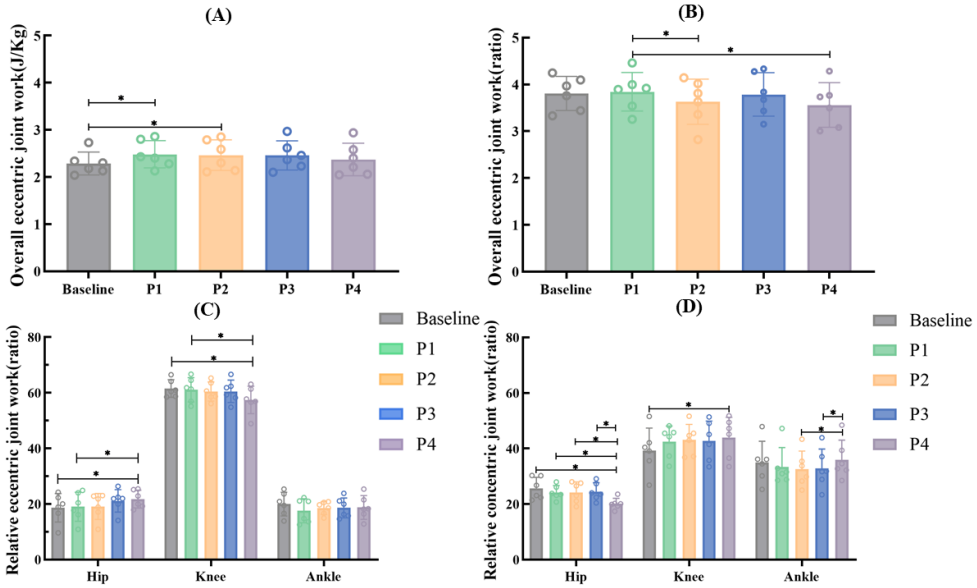

Figure 4. Joint work before and after the Simulated Basketball Game Load (mean and 95% CI). **(A)** Overall eccentric joint work; **(B)** overall concentric joint work; **(C)** relative eccentric joint work; **(D)** relative concentric joint work.
*Statistically significant difference ($p < 0.05$).

3.5. Relationship between each variable

Figure 5 provides a detailed distribution of the *R* values between variables. **Figure 5A** shows the results for the concentric phase variables. **Figure 5B** illustrates the results for the eccentric phase variables. During the eccentric phase, PTF is most influenced by APGRF and knee flexion. In the concentric phase, PTF is most influenced by APGRF, knee extension angular velocity and ankle plantarflexion angular velocity.

The relationships between PTF and other strongly correlated variables are shown in **Figure 6**. PTF correlates positively with knee flexion angle (**Figure 6A**), APGRF in eccentric phase (**Figure 6B**), knee extension angular velocity (**Figure 6C**), ankle dorsiflexion angular velocity (**Figure 6D**), and APGRF in concentric phase (**Figure 6E**), with correlation coefficients (R^2 values) of 0.50, 0.56, 0.70, 0.53, and 0.58 respectively.

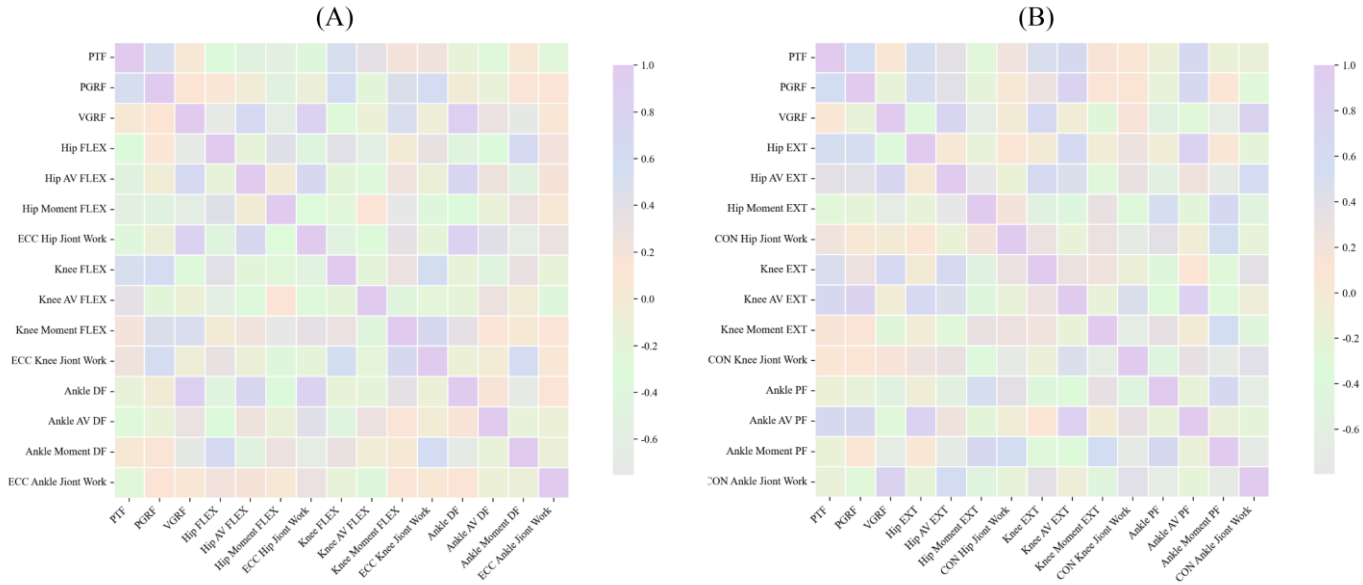

Figure 5. Detailed distributions of absolute value of the correlation coefficient R between variables. **(A)** Detailed distribution of correlation coefficients R between variables during the eccentric phase; **(B)** detailed distribution of correlation coefficients R between variables during the concentric phase.

The closer the R value is to 1, the stronger the correlation between the two variables. The closer the R value is to 0, the weaker the correlation between the two variables.

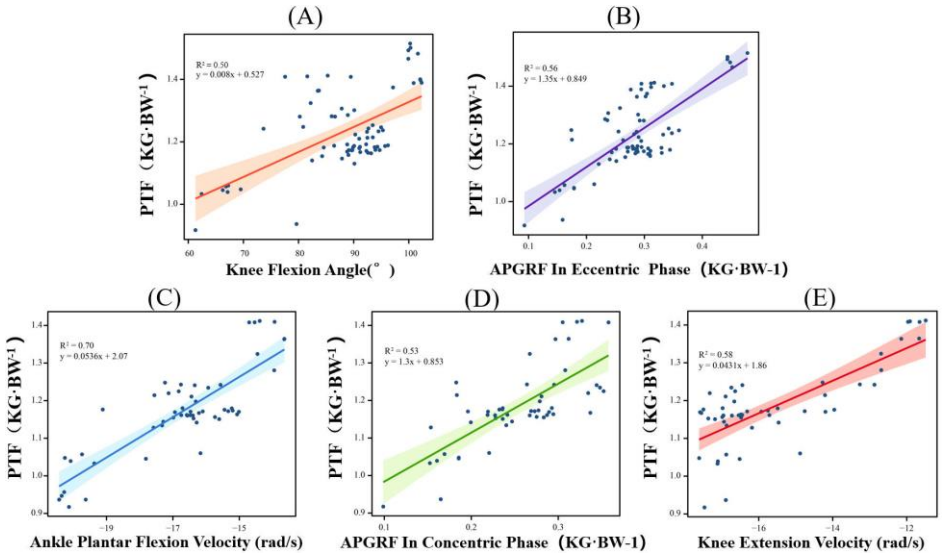

Figure 6. The linear relationships between PTF and other strongly correlated variables are. **(A)** PTF and knee flexion angle during the eccentric phase; **(B)** PTF and anterior-posterior ground reaction force (APGRF) during the eccentric phase; **(C)** PTF and ankle dorsiflexion during the concentric phase; **(D)** PTF and anterior-posterior ground reaction force (APGRF) during the concentric phase; **(E)** PTF and angular velocity of knee extension during the concentric phase.

4. Discussion

This study intends to assess how various stages of simulated basketball game loads impact the patellar tendon during stop-jump tasks and to analyze changes in landing strategies. The results indicate that as the load accumulates, the force exerted

on the patellar tendon decreases, and overall joint work also diminishes. During the eccentric phase, the contribution of knee joint work decreases, while the contribution of hip joint work increases. Conversely, during the concentric phase, the contribution of knee joint work increases, while the contribution of hip joint work decreases. Additionally, the study found that peak PTF almost always occurs at maximum knee flexion. There is a strong correlation between PTF and APGRF (**Figure 6B** and **Figure 6D**).

In the high-intensity simulated basketball game protocol, although the load varied across the five stages, there was no significant impact on VGRF. This finding supports previous research indicating that VGRF is not a reliable indicator of PTF [2]. In other words, using VGRF as a proxy for PTF could lead to the erroneous conclusion that load accumulation during horizontal landing increases patellar tendon load, while in reality, the patellar tendon load decreases (**Table 3**). The study found that compared to the Baseline, P1, and P2 stages, PTF significantly decreased during the P3 and P4 stages, with noticeable changes in landing strategies (**Figure 3**, **Table 3**). The study's hypotheses and conclusions are generally consistent: patellar tendon load decreases in the second and fourth stages, increases in the third stage, and reaches its lowest point in the P4. It is important to note that while a reduction in patellar tendon load was observed in athletes with healthy tendons, this phenomenon may not be observed in asymptomatic athletes. The latter may not adapt to changes induced by fatigue, resulting in unchanged or increased patellar tendon load [14,15]. Previous studies on fatigue protocols have indicated that the peak force exerted on the patellar tendon typically drops to an average of 1.3 times body weight after experiencing fatigue [3,5]. This study found that during the second half of the simulated basketball game, in the P3 and P4, patellar tendon load decreased throughout the landing phase, with average differences ranging from 1.2 to 1.5 times body weight. This finding is comparable to the patellar tendon load observed during horizontal landing phases as modeled by OpenSim [12], with the greatest differences noted during the eccentric landing phase. From a clinical perspective, when patellar tendon load is reduced to 0.7 times body weight, there is a significant reduction in patellar tendon pain, amounting to a decrease of 2.8 points [20]. While this study did not involve injured athletes and acknowledges that pain does not have a complete correlation with tendon load [18,41], the findings imply that accumulated load can mitigate the load on the patellar tendon in healthy basketball players. This decrease could help lower the likelihood of developing PT. Therefore, athletes should incorporate jump exercises that simulate the load patterns observed in this study into their training. This can help improve neuromuscular control during the landing phase. By gradually increasing the intensity of these exercises, athletes can better adapt to the high-load conditions encountered in actual games, thereby reducing the risk of overuse and injury to the patellar tendon.

This study found a strong correlation between PTF and APGRF during the concentric phase (**Table 3**, **Figure 6**). Previous research conducted by Edwards has investigated how muscle fatigue in the lower limbs affects landing techniques and the load on the patellar tendon during stop-jump tasks, finding that PTF significantly decreased while APGRF increased under fatigue conditions [3]. Our study partially confirms these findings. This phenomenon can be explained by the relationship between force and reaction force. During the concentric phase of a stop-jump, PTF

primarily acts on the knee joint to help control and decelerate the body's vertical movement. Meanwhile, APGRF mainly acts on the horizontal plane to control the body's forward and backward movement. After fatigue, the reduction in PTF leads to decreased control in the vertical direction. Consequently, the body may increase horizontal force to maintain balance and complete the movement.

To lessen the load on the patellar tendon during periods of heavy exertion, athletes can utilize both localized and non-local strategies. As a local strategy, the reduction in PTF might result from a decrease in knee joint moment. In this study, a decrease in the knee joint moment was noted during the P2 and P4 of the BEST protocol, likely attributable to the effects of muscle fatigue. This fatigue prevents athletes from generating sufficient knee extension moment, leading to stiffer knee landing movements to prevent knee collapse. Although stiffer landing postures may increase knee joint stability, athletes compensate during the concentric phase by increasing knee joint workload by approximately 5% to achieve the required jump height. Additionally, non-local proximal compensation may help reduce PTF under load accumulation conditions. The control of neuromuscular activity in the proximal parts of the body is essential for both the onset and prevention of lower limb injuries during tasks that involve jumping and landing [42]. Thus, during the eccentric landing phase, the hip joint's workload increased by approximately 3.14% to compensate for the knee joint's workload reduction of 4.09% (**Figure 4C**). The reduction in the maximum hip flexion angle coupled with an increase in the velocity of hip flexion indicates that the body may be trying to make up for decreased strength and flexibility by enhancing the speed of movement when under high-load conditions. This could be a compensatory mechanism to maintain performance. This compensation mechanism aims to maintain movement speed and efficiency. Furthermore, fatigue may lead to a decline in muscle control, making it difficult for athletes to maintain normal movement patterns and force output. In such cases, increasing joint velocity might be the body's way of adapting to fatigue, although this could raise the risk of injury. Overall, proximal compensation is vital for absorbing landing impact loads, especially when distal joints exhibit stiffer movements [4,42]. Basketball players appear to use a combination of localized and broader adaptive strategies, such as proximal compensation and landing with a stiffer lower limb, to alleviate the load on the patellar tendon during high-load scenarios. Recovery strategies should also be adjusted to include sufficient rest and recovery time between training sessions, especially after high-intensity workouts that involve repetitive jumping and landing tasks. This is crucial for allowing the patellar tendon and surrounding tissues to repair and adapt to the imposed loads, reducing the likelihood of developing tendinopathy.

Compared to non-loaded conditions, knee joint moments significantly decrease under load accumulation (**Table 3**), which is the primary reason for the significant reduction in PTF during horizontal landing. We hypothesize that the decrease in knee joint moments is due to changes in the direction and position of various body parts, altering the direction of the ground reaction force vector. This alteration is marked by a landing technique with reduced knee and hip flexion during the horizontal landing phase, which necessitates a lesser forward shift in the center of mass than what is observed under non-loaded conditions. This adjustment helps in managing the impact forces more effectively. Using this landing strategy under high-intensity load

conditions results in lower efficiency in utilizing the stretch-shortening cycle (SSC), preventing participants from generating sufficient net knee extension moments during landing. The earlier studies have shown that adopting smaller knee and hip flexion angles upon landing results in a significantly reduced net knee extension moment, which can be beneficial in minimizing the stress on the knee joint [19]. The lower net knee extension moment may be due to the peak activation of the vastus lateralis (VL) occurring after the PTF, which may in turn result in a reduced knee extension moment. Additionally, the peak activations of the gluteus maximus (MG) and biceps femoris (BF) occurring after the PTF may contribute to lower flexion-extension moments.

In our study, it was observed that the maximum angular velocity of the knee flexion during the horizontal landing phase in the P2 and P4 stages of the BEST protocol was notably higher than the angular velocity recorded during the Baseline (warm-up), indicating a significant increase in the speed of knee flexion under the influence of fatigue from the high-load conditions of the BEST (**Table 2**). Previous studies have demonstrated that during knee flexion upon landing, the patellar tendon experiences both elongation and an increase in tension. Eccentric muscle actions, where the muscle lengthens while generating force, can produce forces up to three times greater than those seen in concentric contractions, where the muscle shortens [43]. Higher stretch velocities typically lead to greater tendon and muscle strain. Repeated exposure to high-speed eccentric loading is often identified as a major cause of cumulative microtrauma in tendons, leading to tendinopathy [44]. During the horizontal landing phase, particularly with rapid repetitive stretching, the risk of tendon inflammation increases, and the risk of patellar tendinopathy is highest during eccentric landing phases. As the load increases, we observed a gradual decrease in knee flexion angles during the third and fourth stages. Landing with smaller knee flexion angles may also result in increased quadriceps force, thereby increasing patellar tendon strain.

This study only includes 16 male amateur basketball players, which is a small sample size. Additionally, the experiment was conducted in a laboratory setting, which may not fully replicate the complex conditions of actual games. It is recommended that future research increase the sample size to include basketball players of different genders, ages, and skill levels, and conduct long-term follow-up studies to observe the long-term effects of load accumulation on patellar tendon stress and injury.

5. Conclusion

This study examined how the various phases of the BEST impact athletes' landing techniques and PTF. The results indicated that, with the accumulation of load, PTF significantly decreased during the P3 and P4, reaching its lowest value in the P4. Simultaneously, the flexion angles of the hip and knee joints significantly decreased, with a reduction in the contribution of eccentric work and an increase in the contribution of concentric work at the knee joint. The reduction in PTF was primarily attributed to participants adjusting their landing techniques, including reducing the flexion angles of the hip and knee joints and decreasing the net knee extension moment. This reduction in PTF during fatigue-induced changes in landing technique may represent an inherent protective strategy, potentially reducing tendon load during

repetitive landings. Encourage athletes to adopt techniques that minimize excessive knee and hip flexion angles and reduce the net knee extension moment during stop-jump movement. training programs should emphasize exercises that strengthen the muscles around the knee joint, particularly focusing on enhancing the eccentric strength of the quadriceps. Implement targeted strength training exercises to enhance the musculature around the knee and hip, improving overall joint stability and control. Emphasizing eccentric strengthening exercises for the quadriceps and hamstrings can help manage the loads transmitted through the patellar tendon.

Author contributions: Conceptualization, DW and FL; methodology, DW; software, FL; validation, DW, FL, JY and JSB; formal analysis, PZ and JY; investigation, DW; resources, ZL; data curation, DW and JY; writing—original draft preparation, DW; writing—review and editing, DW, FL, ML; visualization, FL, JSB, ML; supervision, ML; project administration, ML; funding acquisition, ML. All authors have read and agreed to the published version of the manuscript.

Funding: This study was sponsored by Zhejiang Province Science Fund for Distinguished Young Scholars (Grant number: LR22A020002), Ningbo Key Research and Development Program (Grant number: 2022Z196), Zhejiang Rehabilitation Medical Association Scientific Research Special Fund (ZKKY2023001), Research Academy of Medicine Combining Sports, Ningbo (No.2023001), the Project of Ningbo Leading Medical &Health Discipline (No.2022-F15, No.2022-F22), Ningbo Natural Science Foundation (Grant number: 2022J065, 2022J120) and K. C. Wong Magna Fund in Ningbo University.

Ethical approval: The study was conducted in accordance with the Declaration of Helsinki, and approved by the University's of Ethics Committee (RAGH20231105, 5 November 2023). Informed consent was obtained from all subjects involved in the study. Written informed consent has been obtained from the patient(s) to publish this paper.

Conflict of interest: The authors declare no conflict of interest.

References

1. Lian ØB, Engebretsen L, Bahr R. Prevalence of Jumper's Knee among Elite Athletes from Different Sports: A Cross-sectional Study. The American Journal of Sports Medicine. 2005; 33(4): 561–567. doi: 10.1177/0363546504270454
2. Florit D, Pedret C, Casals M, et al. Incidence of Tendinopathy in Team Sports in a Multidisciplinary Sports Club Over 8 Seasons. J Sports Sci Med. 2019;18(4):780–788.
3. Edwards S, Steele Jr, Purdam Cr, et al. Alterations to Landing Technique and Patellar Tendon Loading in Response to Fatigue. Medicine & Science in Sports & Exercise. 2014; 46(2): 330–340. doi: 10.1249/mss.0b013e3182a42e8e
4. Vermeulen S, De Bleecker C, Spanhove V, et al. The effect of fatigue on spike jump biomechanics in view of patellar tendon loading in volleyball. Scandinavian Journal of Medicine & Science in Sports. 2023; 33(11): 2208–2218. doi: 10.1111/sms.14458
5. Feng R, Best TM, Wang L, et al. Knee Movement Characteristics of Basketball Players in Landing Tasks Before Onset of Patellar Tendinopathy: A Prospective Study. Frontiers in Sports and Active Living. 2022; 4. doi: 10.3389/fspor.2022.847945
6. Sprague AL, Smith AH, Knox P, et al. Modifiable risk factors for patellar tendinopathy in athletes: a systematic review and meta-analysis. British Journal of Sports Medicine. 2018; 52(24): 1575–1585. doi: 10.1136/bjsports-2017-099000
7. van der Worp H, van Ark M, Roerink S, et al. Risk factors for patellar tendinopathy: a systematic review of the literature. British Journal of Sports Medicine. 2011; 45(5): 446–452. doi: 10.1136/bjsm.2011.084079

8. Zhang D, Lyu B, Wu J, et al. Effect of boxers' social support on mental fatigue: Chain mediating effects of coach leadership behaviors and psychological resilience. Work. 2023; 76(4): 1465–1479. doi: 10.3233/wor-220478
9. Wang M, Lyu B. Effect of 24-form simplified Tai Chi on executive inhibitory control of college students: a randomized controlled trial of EEG. Frontiers in Psychology. 2024; 15. doi: 10.3389/fpsyg.2024.1344989
10. Decker MJ, Torry MR, Wyland DJ, et al. Gender differences in lower extremity kinematics, kinetics and energy absorption during landing. Clin Biomech (Bristol, Avon). 2003;18(7):662–669.
11. Devita P, Skelly WA. Effect of landing stiffness on joint kinetics and energetics in the lower extremity. Medicine & Science in Sports & Exercise. 1992; 24(1). doi: 10.1249/00005768-199201000-00018
12. Garcia S, Delattre N, Berton E, et al. Patellar Tendon Force Differs Depending on Jump-Landing Tasks and Estimation Methods. Applied Sciences. 2022; 12(1): 488. doi: 10.3390/app12010488
13. Edwards S, Steele JR, Cook JL, et al. Characterizing patellar tendon loading during the landing phases of a stop‐jump task. Scandinavian Journal of Medicine & Science in Sports. 2012; 22(1): 2–11. doi: 10.1111/j.1600-0838.2010.01119.x
14. Edwards S, Steele JR, Mcghee DE, et al. Landing Strategies of Athletes with an Asymptomatic Patellar Tendon Abnormality. Medicine & Science in Sports & Exercise. 2010; 42(11): 2072–2080. doi: 10.1249/mss.0b013e3181e0550b
15. Mann KJ, Edwards S, Drinkwater EJ, et al. A Lower Limb Assessment Tool for Athletes at Risk of Developing Patellar Tendinopathy. Medicine & Science in Sports & Exercise. 2013; 45(3): 527–533. doi: 10.1249/mss.0b013e318275e0f2
16. Bisseling RW, Hof AL, Bredeweg SW, et al. Are the take-off and landing phase dynamics of the volleyball spike jump related to patellar tendinopathy? British Journal of Sports Medicine. 2008; 42(6): 483–489. doi: 10.1136/bjsm.2007.044057
17. Harris M, Schultz A, Drew MK, et al. Thirty-seven jump-landing biomechanical variables are associated with asymptomatic patellar tendon abnormality and patellar tendinopathy: A systematic review. Physical Therapy in Sport. 2020; 45: 38–55. doi: 10.1016/j.ptsp.2020.03.011
18. Yue Y, Lam WK, Jiang L, et al. The effect of arch-support insole on knee kinematics and kinetics during a stop-jump maneuver. Prosthetics & Orthotics International. 2022; 46(4): 368–373. doi: 10.1097/pxr.0000000000000103
19. Edwards S, Steele JR, Cook JL, et al. Lower Limb Movement Symmetry Cannot Be Assumed When Investigating the Stop–Jump Landing. Medicine & Science in Sports & Exercise. 2012; 44(6): 1123–1130. doi: 10.1249/mss.0b013e31824299c3
20. Silva RS., Purdam CR, Fearon AM, et al. Effects of Altering Trunk Position during Landings on Patellar Tendon Force and Pain. Medicine & Science in Sports & Exercise. 2017; 49(12): 2517–2527. doi: 10.1249/mss.0000000000001369
21. Rudavsky A, Cook J. Physiotherapy management of patellar tendinopathy (jumper's knee). Journal of Physiotherapy. 2014; 60(3): 122–129. doi: 10.1016/j.jphys.2014.06.022
22. Wiesinger HP, Seynnes OR, Kösters A, et al. Mechanical and Material Tendon Properties in Patients With Proximal Patellar Tendinopathy. Frontiers in Physiology. 2020; 11. doi: 10.3389/fphys.2020.00704
23. Ekstrand J, Hägglund M, Waldén M. Epidemiology of Muscle Injuries in Professional Football (Soccer). The American Journal of Sports Medicine. 2011; 39(6): 1226–1232. doi: 10.1177/0363546510395879
24. Powers CM. The Influence of Abnormal Hip Mechanics on Knee Injury: A Biomechanical Perspective. Journal of Orthopaedic & Sports Physical Therapy. 2010; 40(2): 42–51. doi: 10.2519/jospt.2010.3337
25. Harris M, Schultz A, Drew MK, et al. Jump‐landing mechanics in patellar tendinopathy in elite youth basketballers. Scandinavian Journal of Medicine & Science in Sports. 2020; 30(3): 540–548. doi: 10.1111/sms.13595
26. Purdam CR, Cook JL, Hopper DM, Khan KM. Discriminative ability of functional loading tests for adolescent jumper's knee. Physical Therapy in Sport. 2003; 4:3–9.
27. Scanlan AT, Dascombe BJ, Reaburn PR. The Construct and Longitudinal Validity of the Basketball Exercise Simulation Test. Journal of Strength and Conditioning Research. 2012; 26(2): 523–530. doi: 10.1519/jsc.0b013e318220dfc0
28. Hamner SR, Delp SL. Muscle contributions to fore-aft and vertical body mass center accelerations over a range of running speeds. Journal of Biomechanics. 2013; 46(4): 780–787. doi: 10.1016/j.jbiomech.2012.11.024
29. Rajagopal A, Dembia CL, DeMers MS, et al. Full-Body Musculoskeletal Model for Muscle-Driven Simulation of Human Gait. IEEE Transactions on Biomedical Engineering. 2016; 63(10): 2068–2079. doi: 10.1109/tbme.2016.2586891
30. Li F, Zhou H, Xu D, et al. Comparison of Biomechanical Characteristics during the Second Landing Phase in Female Latin Dancers: Evaluation of the Bounce and Side Chasse Step. Molecular & Cellular Biomechanics. 2022;51(10):1977–1986.
31. Cai L, Yan S, Ouyang C, et al. Muscle synergies in joystick manipulation. Frontiers in Physiology. 2023; 14. doi: 10.3389/fphys.2023.1282295

32. Xu D, Lu Z, Shen S, et al. Ugbolue U, Gu Y. The Differences in Lower Extremity Joints Energy Dissipation Strategy during Landing between Athletes with Symptomatic Patellar Tendinopathy (PT) and without Patellar Tendinopathy (UPT). Molecular & Cellular Biomechanics. 2021; 18(2): 107–118. doi: 10.32604/mcb.2021.015453
33. Benítez-Martínez JC, Valera-Garrido F, Martínez-Ramírez P, et al. Lower Limb Dominance, Morphology, and Sonographic Abnormalities of the Patellar Tendon in Elite Basketball Players: A Cross-Sectional Study. Journal of Athletic Training. 2019; 54(12): 1280–1286. doi: 10.4085/1062-6050-285-17
34. Hutchison MK, Houck J, Cuddeford T, et al. Prevalence of Patellar Tendinopathy and Patellar Tendon Abnormality in Male Collegiate Basketball Players: A Cross-Sectional Study. Journal of Athletic Training. 2019; 54(9): 953–958. doi: 10.4085/1062-6050-70-18
35. Peebles AT, Miller TK, Savla J, et al. Reduction of risk factors for ACL Re-injuries using an innovative biofeedback approach: A phase I randomized clinical trial. Physical Therapy in Sport. 2022; 57: 78–88. doi: 10.1016/j.ptsp.2022.07.007
36. Delp SL, Anderson FC, Arnold AS, et al. OpenSim: Open-Source Software to Create and Analyze Dynamic Simulations of Movement. IEEE Transactions on Biomedical Engineering. 2007; 54(11): 1940–1950. doi: 10.1109/tbme.2007.901024
37. DeMers MS, Pal S, Delp SL. Changes in tibiofemoral forces due to variations in muscle activity during walking. Journal of Orthopaedic Research. 2014; 32(6): 769–776. doi: 10.1002/jor.22601
38. Pataky TC, Vanrenterghem J, Robinson MA. Zero- vs. one-dimensional, parametric vs. non-parametric, and confidence interval vs. hypothesis testing procedures in one-dimensional biomechanical trajectory analysis. Journal of Biomechanics. 2015; 48(7): 1277–1285. doi: 10.1016/j.jbiomech.2015.02.051
39. Schober P, Boer C, Schwarte LA. Correlation Coefficients: Appropriate Use and Interpretation. Anesthesia & Analgesia. 2018; 126(5): 1763–1768. doi: 10.1213/ane.0000000000002864
40. Di Paolo S, Nijmeijer E, Bragonzoni L, et al. Comparing lab and field agility kinematics in young talented female football players: Implications for ACL injury prevention. European Journal of Sport Science. 2022; 23(5): 859–868. doi: 10.1080/17461391.2022.2064771
41. Sancho I, Willy RW, Morrissey D, et al. Achilles tendon forces and pain during common rehabilitation exercises in male runners with Achilles tendinopathy. A laboratory study. Physical Therapy in Sport. 2023; 60: 26–33. doi: 10.1016/j.ptsp.2023.01.002
42. De Bleecker C, Vermeulen S, De Blaiser C, et al. Relationship Between Jump-Landing Kinematics and Lower Extremity Overuse Injuries in Physically Active Populations: A Systematic Review and Meta-Analysis. Sports Medicine. 2020; 50(8): 1515–1532. doi: 10.1007/s40279-020-01296-7
43. Vincent KR, Vasilopoulos T, Montero C, et al. Eccentric and Concentric Resistance Exercise Comparison for Knee Osteoarthritis. Medicine & Science in Sports & Exercise. 2019; 51(10): 1977–1986. doi: 10.1249/mss.0000000000002010
44. Babakhani F, Hatefi M, Balochi R. Is there a relationship between isometric hamstrings-to-quadriceps torque ratio and athletes' plyometric performance? PLOS ONE. 2023; 18(11): e0294274. doi: 10.1371/journal.pone.0294274